

# Beam-Helicity Asymmetries in Double-Pion Photoproduction off the Proton

D. Krambrich,<sup>1</sup> F. Zehr,<sup>2</sup> A. Fix,<sup>18</sup> L. Roca,<sup>19</sup> P. Aguar,<sup>1</sup> J. Ahrens,<sup>1</sup> J. R. M. Annand,<sup>3</sup> H. J. Arends,<sup>1</sup> R. Beck,<sup>1,4</sup> V. Bekrenev,<sup>5</sup> B. Boillat,<sup>2</sup> A. Braghieri,<sup>6</sup> D. Branford,<sup>7</sup> W. J. Briscoe,<sup>8</sup> J. Brudvik,<sup>9</sup> S. Cherepnaya,<sup>10</sup> R. Codling,<sup>3</sup> E. J. Downie,<sup>3</sup> P. Dexler,<sup>11</sup> D. I. Glazier,<sup>7</sup> P. Grabmayr,<sup>12</sup> R. Gregor,<sup>11</sup> E. Heid,<sup>1</sup> D. Hornidge,<sup>13</sup> O. Jahn,<sup>1</sup> V. L. Kashevarov,<sup>10</sup> A. Knezevic,<sup>14</sup> R. Kondratiev,<sup>15</sup> M. Korolija,<sup>14</sup> M. Kotulla,<sup>2</sup> B. Krusche,<sup>2</sup> A. Kulbardis,<sup>5</sup> M. Lang,<sup>1,4</sup> V. Lisin,<sup>15</sup> K. Livingston,<sup>3</sup> S. Lugert,<sup>11</sup> I. J. D. MacGregor,<sup>3</sup> D. M. Manley,<sup>16</sup> M. Martinez,<sup>1</sup> J. C. McGeorge,<sup>3</sup> D. Mekterovic,<sup>14</sup> V. Metag,<sup>11</sup> B. M. K. Nefkens,<sup>9</sup> A. Nikolaev,<sup>1,4</sup> P. Pedroni,<sup>6</sup> F. Pheron,<sup>2</sup> A. Polonski,<sup>15</sup> S. N. Prakhov,<sup>9</sup> J. W. Price,<sup>9</sup> G. Rosner,<sup>3</sup> M. Rost,<sup>1</sup> T. Rostomyan,<sup>6</sup> S. Schumann,<sup>1,4</sup> D. Sober,<sup>17</sup> A. Starostin,<sup>9</sup> I. Supek,<sup>14</sup> C. M. Tarbert,<sup>7</sup> A. Thomas,<sup>1</sup> M. Unverzagt,<sup>1,4</sup> Th. Walcher,<sup>1</sup> and D. P. Watts<sup>7</sup>

(Crystal Ball at MAMI, TAPS, and A2 Collaborations)

<sup>1</sup>*Institut für Kernphysik, Johannes Gutenberg-Universität Mainz, Mainz, Germany*

<sup>2</sup>*Department of Physics, University of Basel, Basel, Switzerland*

<sup>3</sup>*Department of Physics and Astronomy, University of Glasgow, Glasgow, United Kingdom*

<sup>4</sup>*Helmholtz-Institut für Strahlen- und Kernphysik, University Bonn, Bonn, Germany*

<sup>5</sup>*Petersburg Nuclear Physics Institute, Gatchina, Russia*

<sup>6</sup>*INFN Sezione di Pavia, Pavia, Italy*

<sup>7</sup>*School of Physics, University of Edinburgh, Edinburgh, United Kingdom*

<sup>8</sup>*Center for Nuclear Studies, The George Washington University, Washington, D.C., USA*

<sup>9</sup>*University of California at Los Angeles, Los Angeles, California, USA*

<sup>10</sup>*Lebedev Physical Institute, Moscow, Russia*

<sup>11</sup>*II. Physikalisches Institut, University of Giessen, Giessen, Germany*

<sup>12</sup>*Physikalisches Institut Universität Tübingen, Tübingen, Germany*

<sup>13</sup>*Mount Allison University, Sackville, New Brunswick, Canada*

<sup>14</sup>*Rudjer Boskovic Institute, Zagreb, Croatia*

<sup>15</sup>*Institute for Nuclear Research, Moscow, Russia*

<sup>16</sup>*Kent State University, Kent, Ohio, USA*

<sup>17</sup>*The Catholic University of America, Washington, D.C., USA*

<sup>18</sup>*Laboratory of Mathematical Physics, Tomsk Polytechnic University, 634034 Tomsk, Russia*

<sup>19</sup>*Departamento de Física, Universidad de Murcia, Murcia, Spain*

(Received 10 October 2008; revised manuscript received 18 June 2009; published 30 July 2009)

Beam-helicity asymmetries have been measured at the MAMI accelerator in Mainz in the three isospin channels  $\vec{\gamma}p \rightarrow \pi^+ \pi^0 n$ ,  $\vec{\gamma}p \rightarrow \pi^0 \pi^0 p$ , and  $\vec{\gamma}p \rightarrow \pi^+ \pi^- p$ . The circularly polarized photons, produced from bremsstrahlung of longitudinally polarized electrons, were tagged with the Glasgow magnetic spectrometer. Charged pions and the decay photons of  $\pi^0$  mesons were detected in a  $4\pi$  electromagnetic calorimeter which combined the Crystal Ball detector with the TAPS detector. The precisely measured asymmetries are very sensitive to details of the production processes and are thus key observables in the modeling of the reaction dynamics.

DOI: 10.1103/PhysRevLett.103.052002

PACS numbers: 13.60.Le, 14.20.Gk, 14.40.Aq, 25.20.Lj

Double-pion photoproduction allows the study of sequential decays of nucleon resonances via intermediate excited states, as well as the coupling of nucleon resonances to  $N\rho$  and  $N\sigma$ . It has therefore become an attractive tool for the study of the excitation spectrum of the nucleon, which is intimately connected to the properties of QCD in the nonperturbative range. Its contribution to the total electromagnetic response of the nucleon is substantial. In the second resonance region, comprising the  $P_{11}(1440)$ ,  $S_{11}(1535)$ , and  $D_{13}(1520)$  resonances, roughly 50% of the total photoabsorption cross section originates from it. In this energy region total cross sections and invariant mass

distributions of the  $\pi\pi$ -pairs and the  $\pi N$ -pairs have been measured with the DAPHNE and TAPS detectors at the MAMI accelerator in Mainz [1–8], at GRAAL in Grenoble (also linearly polarized beam asymmetry) [9,10], with the CLAS detector at JLab (electroproduction) [11], and at ELSA in Bonn [12,13]. More recently, also polarization observables have been measured at the MAMI accelerator [14–16] and at the CLAS facility at Jlab [17].

In spite of all these efforts, even the interpretation of the data in the energy region, where only few resonances can contribute, is still surprisingly controversial [18] since the available data do not sufficiently constrain the model

analyses. It is thus evident that the search for missing resonances at higher energy requires a better understanding of the reaction mechanisms. The controversy has far reaching consequences not only for the  $N^*$  excitation spectrum itself, but as discussed below also in the field of the much discussed hadron in-medium properties.

There is agreement that the  $\pi^+\pi^-$  final state is dominated by background terms, in particular, of the  $\Delta$ -Kroll-Rudermann type, while  $\pi^0\pi^0$  has only small background contributions and thus is particularly suited for the study of sequential resonance decays. However, even for the latter the results of different reaction models are contradictory. Calculations by the Valencia group [19–21] emphasize a large contribution from the  $D_{13} \rightarrow \Delta\pi^0 \rightarrow p\pi^0\pi^0$  decay. Laget and co-workers [9], instead find a dominant contribution from the  $P_{11}(1440) \rightarrow N\sigma$  decay and a recent analysis by the Bonn-Gatchina group [12,13] reports a strong contribution from the  $D_{33}(1700)$  resonance, which is not seen in other models. Modifications of the invariant mass distributions of the  $\pi^0$  pairs for photoproduction off heavy nuclei have been discussed in view of the predicted  $\sigma$  in-medium modification resulting from partial chiral symmetry restoration [22,23]; however, a better understanding of the elementary production processes is obligatory. Similarly, for the mixed charge channel  $n\pi^+\pi^0$  all early model calculations (see e.g., [19]) failed already in the reproduction of the total cross section. Only the introduction of a strong contribution from the  $\rho$  meson [20,21,24], motivated by the shape of the measured invariant mass distributions [4,7], improved the situation. Again, a close connection to a different problem, namely, the still unexplained strong suppression of the second resonance bump in photoproduction off nuclei (see e.g., [25]) is involved, where a possible explanation might arise from the in-medium modification of the  $D_{13}(1520) \rightarrow N\rho$  decay [7].

Recently, model predictions [21,24,26,27], which indicated that polarization observables are extremely sensitive for the disentanglement of the reaction mechanisms, have triggered wide-spread experimental activities. The advent of accelerators with highly polarized electron beams has provided a new tool for this field: meson photoproduction using circularly polarized photons. They are produced by the bremsstrahlung of longitudinally polarized electrons in an amorphous radiator. The polarization transfer obeys a simple formula given by Olsen and Maximon [28]. The beam-helicity asymmetry can then be measured by comparing the event rates for the two helicity states of the beam. Parity conservation precludes any sensitivity of the cross section in a two-body reaction to beam helicity alone, but in a reaction with three or more particles in the final state, circularly polarized photons can lead to asymmetries even for an unpolarized target. Until recently there was little effort to study these effects until two experimental programs at JLab observed strong signals. In hyperon

photoproduction, the decay of the final state  $\Lambda$  or  $\Sigma$  hyperon has an angular dependence on the hyperon polarization, and a recent experiment [29] has shown that the polarization transfer along the photon momentum axis is nearly 100%. In an analysis of charged double-pion production  $\gamma p \rightarrow p\pi^+\pi^-$  measured with CLAS, Strauch *et al.* [17] found a large helicity asymmetry in the distribution of  $\Phi$ , the angle between the two-pion plane and the  $\gamma p$  reaction plane (see Fig. 1).

The Crystal-Ball-TAPS collaboration at the Mainz microtron MAMI [30] has recently taken data on the photoproduction of the three  $\pi\pi N$  final states accessible with a proton target:  $\gamma p \rightarrow p\pi^+\pi^-$ ,  $\gamma p \rightarrow p\pi^0\pi^0$ , and  $\gamma p \rightarrow n\pi^+\pi^0$ , using circularly polarized photons. This Letter presents the beam-helicity asymmetries in a form similar to that of Strauch *et al.* The data were taken with tagged photons incident on a 4.8 cm long liquid hydrogen target (surface density 0.201 nuclei/barn). Contributions from the target windows ( $2 \times 60 \mu\text{m}$  Kapton) were determined with empty target measurements and subtracted. The photons of up to 820 MeV, were produced by the bremsstrahlung of 883 MeV longitudinally polarized electrons. The energy of the photons was determined by the Glasgow photon tagger [31,32] with a resolution of approximately 2 MeV full width. The target was located inside the Crystal Ball (CB) [33], consisting of 672 NaI crystals that covered the full azimuthal range for polar angles between  $20^\circ$ – $160^\circ$ . The angular region from  $20^\circ$  down to  $1^\circ$  was covered by the TAPS detector [34,35] with 510 BaF<sub>2</sub> crystals arranged as a hexagonal wall. The target was surrounded by a particle identification detector (PID) [36] and two cylindrical multiple wire proportional chambers (MWPCs) [37]. Protons and charged pions hitting the CB were identified by an  $E - \Delta E$  analysis, using the energy information of the CB and the PID. For TAPS, the separation of photons, neutrons, protons, and charged pions can be achieved in principal as discussed in [23]. However, here these methods were only used for a clean identification of photons. Protons and charged pions in TAPS were

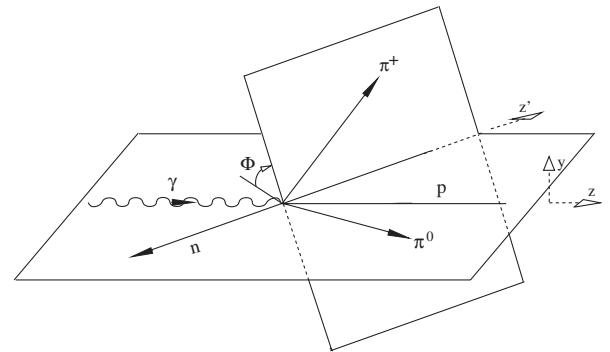


FIG. 1. Vector and angle definitions.  $\Phi$  is the angle between the reaction plane (defined by  $\vec{k}$  and  $\vec{p}_n$ ) and the production plane of the two pions (defined by  $\vec{p}_{\pi^0}$  and  $\vec{p}_{\pi^+}$ ).

not included in the analysis, since their separation was less clean than the  $E - \Delta E$  analysis by PID and CB.

In the first step of the reaction identification for the  $p\pi^0\pi^0$  final state, events with four photons and one or no proton candidate were selected. Similarly, for the  $n\pi^+\pi^0$  final state two photons, a  $\pi^+$ , and one or no neutron were required. The  $\pi^0$  mesons were then identified by a standard invariant mass analysis. Further identification of the reactions was based on missing mass analyses for the recoil nucleons in a manner similar to that described in [5–8]. It was used to remove small residual background from  $\eta \rightarrow 3\pi$  decays, which however, was much less important than in previous experiments, since due to the large solid angle coverage, in most cases the third pion was also seen. For both reactions, the recoil nucleons were treated as missing particles, no matter whether a candidate was found or not, so that the results are independent of the detector acceptance and efficiency for recoil nucleons. This event selection guaranteed full solid angle coverage for the  $\pi^0\pi^0$  channel. For the  $\pi^+\pi^0$  reaction only events with the  $\pi^+$  at laboratory polar angles smaller than  $20^\circ$  (and larger than  $160^\circ$ ) were excluded, which has a negligible effect on the measured asymmetries. Since identification of the double charged channel is missing the powerful tool of invariant mass analysis, in this case detection of all three charged particles was required in order to achieve an equally good background suppression as for the other channels (residual background from  $\gamma p \rightarrow p\pi^+\pi^-\pi^0$  was again removed with a missing mass analysis). This selection means that for the double charged channel only events with all three particles at laboratory polar angles larger than  $20^\circ$  (and smaller than  $160^\circ$ ) were accepted. This limitation was accounted for in the model calculations.

The missing mass spectra for all three reactions were extremely clean and very well reproduced by Monte Carlo simulations. Residual background was estimated at maximum at the few percent level (certainly well below 5% for all channels) and is thus not relevant for any results presented here. Details of the analysis will be discussed in an upcoming paper about total cross sections and invariant mass distributions.

In a reaction produced by circularly polarized photons on an unpolarized target the beam-helicity asymmetry  $I^\circ$  is defined by:

$$I^\circ(\Phi) = \frac{1}{P_\gamma} \frac{d\sigma^+ - d\sigma^-}{d\sigma^+ + d\sigma^-} = \frac{1}{P_\gamma} \frac{N^+ - N^-}{N^+ + N^-}, \quad (1)$$

where  $d\sigma^\pm$  is the differential cross section for each of the two photon helicity states, and  $P_\gamma$  is the degree of circular polarization of the photons. The latter is calculated as a product of the polarization degree of the longitudinally polarized electrons ( $82 \pm 5\%$ ) and the photon-energy-dependent polarization transfer factor [28]. In the energy range of interest,  $P_\gamma$  was between 60% and 80%. Possible

differences in the number of incident photons for the two helicity states have been determined to be at the  $5 \times 10^{-4}$  level; i.e., they are negligible. The angle  $\Phi$  between reaction and production plane is calculated as defined in the work of Roca [27] from the three-momenta of the particles (the same construction was used for the analysis of the CLAS-data [17]). For  $\pi^+\pi^0$  production the two pions are ordered as shown in Fig. 1. For double  $\pi^0$  production and for the double charged state their assignment is randomized since the experiment cannot distinguish positively and negatively charged pions. This means that for the latter two  $I^\circ(\Phi) = I^\circ(\Phi + \pi)$ .

For the extraction of the asymmetry  $I^\circ(\Phi, \Theta_{\pi_1}, \Theta_{\pi_2}, \dots)$  in a limited region of kinematics, the differential cross sections  $d\sigma^\pm$  can be replaced by the respective count rates  $N^\pm$  [right-hand side of Eq. (1)], since all normalization factors cancel in the ratio. In principle, efficiency weighted count rates ought to be used to obtain the angle integrated asymmetries. For the two final states  $\pi^0\pi^0$  and  $\pi^+\pi^0$ , for which also precise total cross sections and invariant mass distributions will be published elsewhere, the detection efficiency was modeled with Monte Carlo simulations. However, since the efficiencies are rather flat functions of the pion polar angles, the effect of the efficiency corrections on the asymmetries was negligible. As in the CLAS experiment, [17] only the raw asymmetries are given for  $\pi^+\pi^-$  production.

The measured asymmetries are summarized in Figs. 2 and 3 as functions of  $\Phi$ . Parity conservation enforces  $I^\circ(\Phi) = -I^\circ(2\pi - \Phi)$ . This condition was not used as a constraint in the analysis but is very well respected, demonstrating the excellent quality of the data.

The asymmetries are compared to the results from the model of Fix and Arenhövel [24] and the Valencia model [27], which were calculated taking into account the acceptance limitations for  $\pi^+\pi^-$  and the fact that  $\pi^-$  could not be distinguished from  $\pi^+$  in the detectors. For this channel also the prediction of the Valencia model for full  $4\pi$  acceptance is shown. At least in the framework of the model, the effect from the acceptance limitation is small. A similar result as in the CLAS experiment [17] is found. The two models make similar predictions, but agree with the measurements only in the energy range around 715 MeV. For  $n\pi^0\pi^+$ , the model results are similar above 700 MeV, but are nowhere in agreement with the data. For the Valencia model [27] also the solution without the  $D_{13} \rightarrow N\rho$  contribution is shown. It was introduced into the model [20,21] in order to reproduce the previously nonunderstood total cross section and pion invariant mass distributions [4,7]. However, in the  $D_{13}$  range, inclusion of this contribution does not at all improve the agreement with the asymmetries. Finally, for  $p\pi^0\pi^0$  Fix's model and the Bonn-Gatchina analysis (not available for the other isospin channels) [12,13] are in fairly good agreement with the data, while the Valencia model is out of phase.

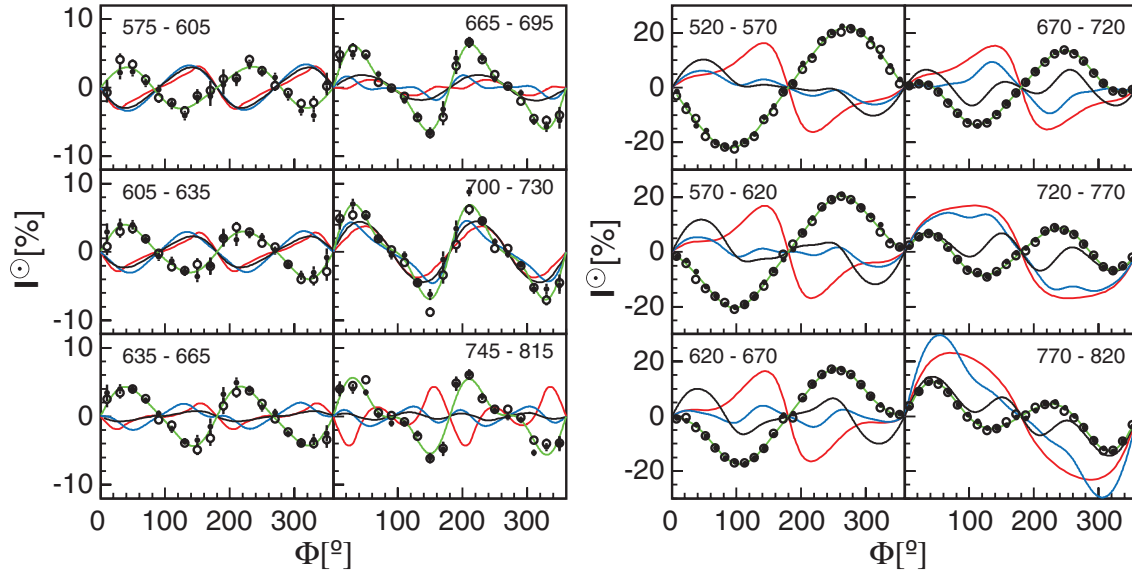


FIG. 2 (color). Left-hand side: Beam-helicity asymmetry in the  $\gamma p \rightarrow p\pi^+\pi^-$  reaction for different bins of photon energy. Filled symbols:  $I^0(\Phi)$ , open symbols:  $-I^0(2\pi - \Phi)$ . Green curves: fit to the data. Red curves: Fix and Arenhövel model [24]; Blue: Roca [27], Black: Roca [27] for  $4\pi$  acceptance. Right-hand side: Beam-helicity asymmetry for  $\gamma p \rightarrow n\pi^+\pi^0$ . Notation as for left-hand side except black curves: Roca [27] without  $D_{13} \rightarrow N\rho$ .

Because of its symmetry,  $I^0(\Phi)$  can be expanded into a sine-series (odd coefficients vanish for identical pions):

$$I^0(\Phi) = \sum_{n=1}^{\infty} A_n \sin(n\Phi). \quad (2)$$

The data have been fitted to Eq. (2) for  $n \leq 4$  (higher orders were not significant), and the results are summarized in Fig. 4. For the  $p\pi^0\pi^0$  and  $p\pi^+\pi^-$  final states the results for the odd terms  $A_1$  and  $A_3$  are consistent with zero, which is additional evidence that no false asymmetries have been generated in the experiment. For comparison, the CLAS results [17] for  $p\pi^+\pi^-$  have also been fitted.

Since in the CLAS experiment negatively and positively charged pions were distinguished, the odd terms can also contribute, but the even terms  $A_2$  and  $A_4$  can be compared to the present results. One must, however, keep in mind that the acceptance was not identical (CLAS covered polar angles down to  $8^\circ$ , this experiment down to  $20^\circ$ ). For  $A_2$  the energy dependence is similar, although the present values are somewhat larger. No significant contribution from  $n = 4$  was found for the CLAS experiment, but in the present measurement it contributes up to 2%. The comparison of the results for the three final states highlights the different reaction mechanisms in the three isospin channels.

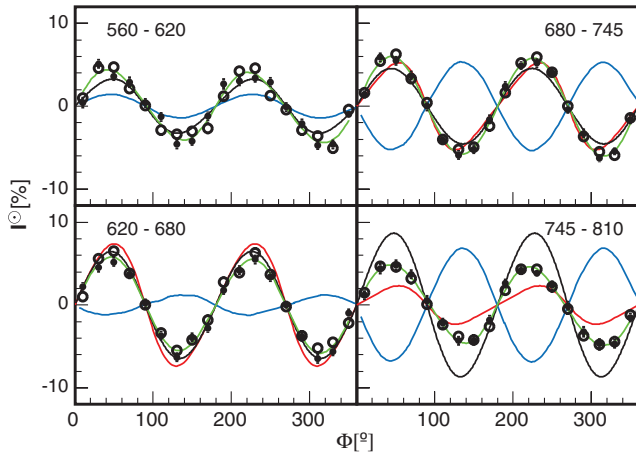


FIG. 3 (color). Beam-helicity asymmetry for  $\gamma p \rightarrow \pi^0\pi^0 p$ . Notation as in Fig. 2 except black curves: Bonn-Gatchina model [12,13].

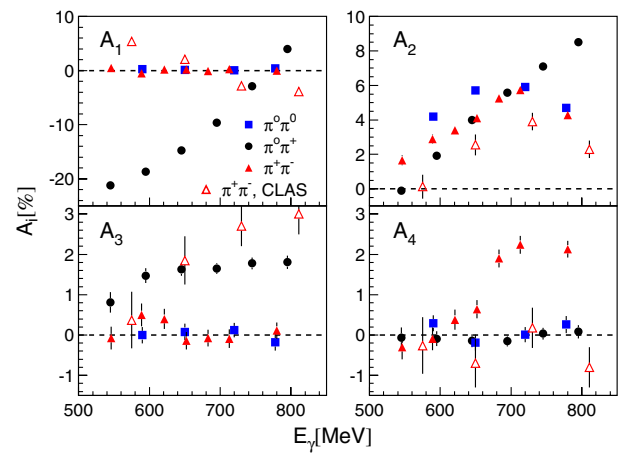


FIG. 4 (color online). Fitted coefficients of the expansion of the beam-helicity asymmetries. Note that the acceptance for the present  $\pi^+\pi^-$  and the CLAS data are different (see text).



In summary, precise measurements of the beam-helicity asymmetry for double-pion photoproduction on the proton have been presented for all three isospin channels. The comparison with model predictions highlights both the challenges and potential rewards for the extraction of resonance properties. On the one hand, the progress in experimental techniques allows precise measurements of this observable, and the predictions for it are very sensitive to the internal mechanisms of the models. On the other hand, the general lack of agreement between experiment and theory signals that significant improvements in the models are needed. The present data can provide rigorous tests for future developments on the way to an eventual reliable extraction of resonance contributions from double-pion photoproduction. The very precise results for the total cross sections, including sensitive measurements of the threshold behavior in view of the predictions of chiral perturbation theory, and the invariant mass distributions of pion-pion and pion-nucleon pairs, which have been extracted with a precision far superior to any previous measurements, will be presented in an upcoming paper.

We wish to acknowledge the outstanding support of the accelerator group and operators of MAMI. This work was supported by Deutsche Forschungsgemeinschaft (SFB 443, SFB/TR 16), DFG-RFBR (Grant No. 05-02-04014), Schweizerischer Nationalfonds, UK Science and Technology Facilities Council (STFC), European Community-Research Infrastructure Activity (FP6), the US DOE, US NSF and NSERC (Canada). We thank the undergraduate students of Mount Allison and George Washington Universities for their assistance.

- 
- [1] A. Braghieri *et al.*, Phys. Lett. B **363**, 46 (1995).
  - [2] F. Härter *et al.*, Phys. Lett. B **401**, 229 (1997).
  - [3] A. Zabrodin *et al.*, Phys. Rev. C **55**, R1617 (1997).
  - [4] A. Zabrodin *et al.*, Phys. Rev. C **60**, 055201 (1999).
  - [5] M. Wolf *et al.*, Eur. Phys. J. A **9**, 5 (2000).
  - [6] V. Kleber *et al.*, Eur. Phys. J. A **9**, 1 (2000).
  - [7] W. Langgärtner *et al.*, Phys. Rev. Lett. **87**, 052001 (2001).
  - [8] M. Kotulla *et al.*, Phys. Lett. B **578**, 63 (2004).
  - [9] Y. Assafiri *et al.*, Phys. Rev. Lett. **90**, 222001 (2003).
  - [10] J. Ajaka *et al.*, Phys. Lett. B **651**, 108 (2007).
  - [11] M. Ripani *et al.*, Phys. Rev. Lett. **91**, 022002 (2003).
  - [12] U. Thoma *et al.*, Phys. Lett. B **659**, 87 (2008).
  - [13] A. V. Sarantsev *et al.*, Phys. Lett. B **659**, 94 (2008).
  - [14] J. Ahrens *et al.*, Phys. Lett. B **551**, 49 (2003).
  - [15] J. Ahrens *et al.*, Phys. Lett. B **624**, 173 (2005).
  - [16] J. Ahrens *et al.*, Eur. Phys. J. A **34**, 11 (2007).
  - [17] S. Strauch *et al.*, Phys. Rev. Lett. **95**, 162003 (2005).
  - [18] B. Krusche and S. Schadmand, Prog. Part. Nucl. Phys. **51**, 399 (2003).
  - [19] J. A. Gomez-Tejedor and E. Oset, Nucl. Phys. A **600**, 413 (1996).
  - [20] J. C. Nacher *et al.*, Nucl. Phys. A **695**, 295 (2001).
  - [21] J. C. Nacher and E. Oset, Nucl. Phys. A **697**, 372 (2002).
  - [22] J. G. Messchendorp *et al.*, Phys. Rev. Lett. **89**, 222302 (2002).
  - [23] F. Bloch *et al.*, Eur. Phys. J. A **32**, 219 (2007).
  - [24] A. Fix and H. Ahrenhövel, Eur. Phys. J. A **25**, 115 (2005).
  - [25] N. Bianchi *et al.*, Phys. Lett. B **325**, 333 (1994).
  - [26] W. Roberts and T. Oed, Phys. Rev. C **71**, 055201 (2005).
  - [27] L. Roca, Nucl. Phys. A **748**, 192 (2005).
  - [28] H. Olsen and L. C. Maximon, Phys. Rev. **114**, 887 (1959).
  - [29] R. K. Bradford *et al.*, Phys. Rev. C **75**, 035205 (2007).
  - [30] Th. Walcher, Prog. Part. Nucl. Phys. **24**, 189 (1990).
  - [31] I. Anthony *et al.*, Nucl. Instrum. Methods Phys. Res., Sect. A **301**, 230 (1991).
  - [32] S. J. Hall, G. J. Miller, R. Beck, and P. Jennewein, Nucl. Instrum. Methods Phys. Res., Sect. A **368**, 698 (1996).
  - [33] A. Starostin *et al.*, Phys. Rev. C **64**, 055205 (2001).
  - [34] R. Novotny, IEEE Trans. Nucl. Sci. **38**, 379 (1991).
  - [35] A. R. Gabler *et al.*, Nucl. Instrum. Methods Phys. Res., Sect. A **346**, 168 (1994).
  - [36] D. Watts, in *Calorimetry in Particle Physics, Proceedings of the 11th International Conference, Perugia, Italy 2004*, edited by C. Cecchi, P. Cenci, P. Lubrano, and M. Pepe (World Scientific, Singapore, 2005), p. 560.
  - [37] G. Audit *et al.*, Nucl. Instrum. Methods Phys. Res., Sect. A **301**, 473 (1991).